

# Better than Nature: Nicotinamide Biomimetics That Outperform Natural Coenzymes

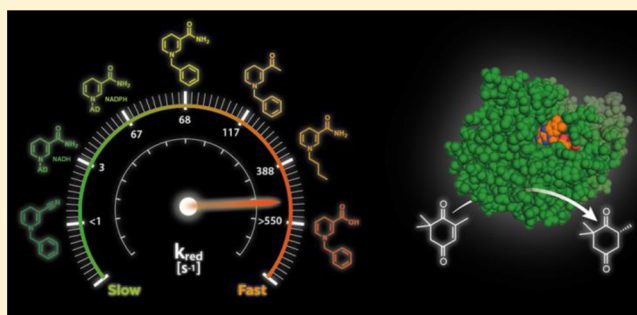
Tanja Knaus,<sup>†,§,||</sup> Caroline E. Paul,<sup>‡,§</sup> Colin W. Levy,<sup>†</sup> Simon de Vries,<sup>‡</sup> Francesco G. Mutti,<sup>†,||</sup> Frank Hollmann,<sup>\*,‡</sup> and Nigel S. Scrutton<sup>\*,†</sup>

<sup>†</sup>BBSRC/EPSCRC Centre for Synthetic Biology of Fine and Speciality Chemicals, Faculty of Life Sciences, Manchester Institute of Biotechnology, 131 Princess Street, Manchester M1 7DN, United Kingdom

<sup>‡</sup>Department of Biotechnology, Delft University of Technology, Julianalaan 136, 2628BL Delft, The Netherlands

## S Supporting Information

**ABSTRACT:** The search for affordable, green biocatalytic processes is a challenge for chemicals manufacture. Redox biotransformations are potentially attractive, but they rely on unstable and expensive nicotinamide coenzymes that have prevented their widespread exploitation. Stoichiometric use of natural coenzymes is not viable economically, and the instability of these molecules hinders catalytic processes that employ coenzyme recycling. Here, we investigate the efficiency of man-made synthetic biomimetics of the natural coenzymes NAD(P)H in redox biocatalysis. Extensive studies with a range of oxidoreductases belonging to the “ene” reductase family show that these biomimetics are excellent analogues of the natural coenzymes, revealed also in crystal structures of the ene reductase XenA with selected biomimetics. In selected cases, these biomimetics outperform the natural coenzymes. “Better-than-Nature” biomimetics should find widespread application in fine and specialty chemicals production by harnessing the power of high stereo-, regio-, and chemoselective redox biocatalysts and enabling reactions under mild conditions at low cost.



## INTRODUCTION

Through the process of natural selection, Nature has evolved well-adapted macromolecular structures that interact with biological small molecules. Oxidoreductases, for example, rely on the nicotinamide coenzymes to supply them with the redox equivalents required to sustain their catalytic cycles. Two forms of natural coenzymes exist: the phosphorylated ( $\text{NADP}^+/\text{NADPH}$ ) and nonphosphorylated ( $\text{NAD}^+/\text{NADH}$ ) forms (Figure 1A). Nicotinamide coenzymes essentially contain two structural motifs, the nicotinamide moiety conferring their electrochemical function (i.e., serving as an electron source or sink in the form of a hydride) and the adenosine dinucleotide moiety conferring the separation between anabolic and catabolic pathways. NADP is involved in anabolic redox processes, whereas NAD is mostly found in processes dealing with energy metabolism. While this separation between different metabolic pathways is essential for cellular survival, it is irrelevant in chemical applications of redox enzymes. Therefore, there is a renewed interest in the design of simple synthetic analogues of the natural nicotinamide coenzymes. The laboratory-based design and synthesis of small molecule biomimetics that can functionally substitute (or even outperform) those available in Nature is a major challenge. The development of biomimetics that can be synthesized easily and exploited widely would be a game changer in establishing new manufacturing technologies that would be too expensive using

natural biological molecules. The natural coenzymes NAD(P)H are prohibitively expensive and chemically too unstable for stoichiometric use in fine and specialty chemicals manufacture. This has prevented their general uptake as a source of reducing equivalents in biocatalytic oxidoreductase-catalyzed reactions and has led to the development of in situ regeneration systems to replenish NAD(P)H (e.g., using enzymatic, photochemical, and electrochemical approaches<sup>1–5</sup>) or the use of hydrogen-borrowing biocatalytic cascades.<sup>6–9</sup> In turn, the limited stability and expense of natural nicotinamide coenzymes have driven a search for more stable synthetic nicotinamide coenzyme analogues that can interface generally with biological oxidoreductase catalysts.<sup>10</sup>

Nicotinamide-dependent biocatalysts have wide-ranging potential in biocatalytic transformations. Ene reductases (ERs) from the Old Yellow Enzyme family (EC 1.3.1.31) are particularly attractive as they are a group of broad specificity biocatalysts that catalyze the asymmetric reduction of activated C=C bonds, forming up to two new stereogenic centers at the expense of the natural nicotinamide coenzyme NAD(P)H as an electron source.<sup>11–13</sup> In particular,  $\alpha,\beta$ -unsaturated carbonyl compounds (e.g., enals and enones) and nitroalkenes are excellent substrates.<sup>14–17</sup> In general,  $\alpha,\beta$ -unsaturated diesters as

Received: November 23, 2015

Published: January 3, 2016

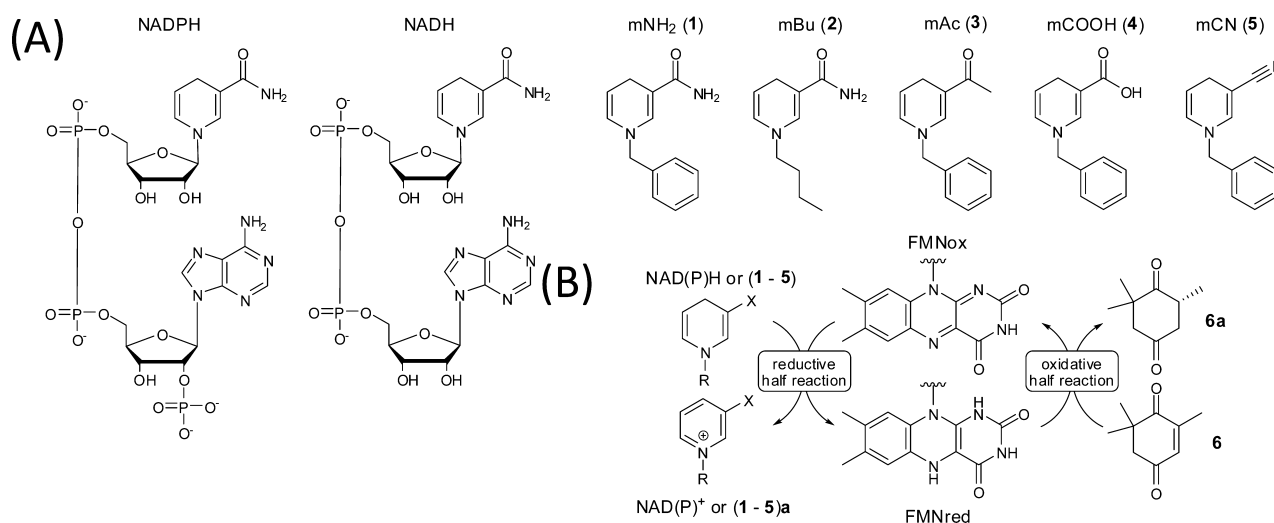


**Figure 1.** (A) Structure of NAD(P)H and synthetic nicotinamide biomimetic mNADHs (1–5) and (B) the catalytic cycle of ER-catalyzed reactions.

well as  $\alpha,\beta$ -unsaturated diacids are also reduced by ERs.<sup>18</sup> In contrast, the efficient reduction of  $\alpha,\beta$ -unsaturated monoacids or monoesters requires an additional electron-withdrawing group in the  $\alpha$ - or  $\beta$ -position in order to activate the alkene moiety.<sup>19–22</sup> The ability to form new stereogenic centers and the wide acceptance of different substrate types are driving the exploitation of ERs toward novel applications in redox biocatalysis and implementation in key industrial processes.<sup>22–25</sup> ERs have been studied extensively over the past decade, and there is detailed information known, such as their structure, reaction mechanism, substrate scope, kinetic properties, and biocatalytic approaches.<sup>26,27,13</sup> The catalytic cycle of ER-catalyzed reactions can be divided into two separated half-reactions: in the reductive half-reaction, a hydride is transferred from NAD(P)H to the enzyme-bound flavin (flavin mononucleotide; FMN). After release of oxidized NAD(P)<sup>+</sup>, this hydride is then transferred in the oxidative half-reaction from the flavin N5 position to the activated alkene substrate (Figure 1B).<sup>28–30</sup>

Recently, nicotinamide coenzyme biomimetics (mNADHs) were shown to replace NAD(P)H in ER-catalyzed reactions.<sup>10</sup> A series of mNADHs (1–5) has been synthesized to replace the natural coenzymes for various ERs (Figure 1A). These coenzyme biomimetics show great promise and have sparked renewed interest in redox biocatalysis.<sup>1,31</sup> In addition, reduction of C=C double bonds<sup>10</sup> and oxyfunctionalization reactions such as epoxidation<sup>32</sup> or hydroxylation<sup>33–35</sup> using mNADHs have been reported. However, structural–mechanistic understanding of biomimetic chemistry in ER-catalyzed reactions is lacking, preventing the successful exploitation of these biomimetics. This information can be derived from knowledge of crystal structures of enzyme–biomimetic complexes and analysis of reaction cycle kinetics, both presented here for the first time for a panel of structurally diverse nicotinamide biomimetics in combination with several ERs. These structural–mechanistic analyses show how selected biomimetics perform as well and, in some cases, even outperform the natural coenzymes. The chemical stability of the biomimetics, coupled with their enhanced enzymatic reactivity, gives rise to the rare situation where chemical designs surpass those available in the natural world. These biomimetics provide an attractive means of performing redox biotransformations with

ERs (and *mutatis mutandis* other redox biocatalysts) under mild reaction conditions and at relatively low cost.

## RESULTS AND DISCUSSION

We set out to determine the structures of selected complexes formed between ER biocatalysts and the biomimetics to ascertain if the biomimetic design features replicate those seen for the natural enzyme–coenzyme complexes. The tetrahydro forms of the natural (NADPH<sub>4</sub>) and biomimetic (mNADH<sub>4</sub>s) ligands were used to prevent hydride transfer in the crystal complexes (Figure 2).<sup>36,37</sup> Crystal structures were determined for XenA in complex with NADPH<sub>4</sub> and tetrahydro-biomimetics (1b, 2b, and 3b) at 1.6–1.8 Å resolution. Clear electron density was observed for the bound NADPH<sub>4</sub> extending from the nicotinamide moiety and becoming disordered after the diphosphate moieties. NADPH<sub>4</sub> binds in a stacked arrangement sitting above the isoalloxazine ring of the FMN cofactor, and His181 and His178 are located 2.8 and 2.9 Å, respectively, from the nicotinamide oxygen, with Cys25 some 3.6 Å from the nicotinamide N7 position. Each of the three bound biomimetics occupies the same region of the active site as that observed for NADPH<sub>4</sub> (Figure 2), with only very minimal changes observed in the positions of surrounding residues in the active site. However, the reduced bulk of the biomimetics when compared to the dinucleotide portion of NADPH<sub>4</sub> (Figure 2) results in Trp302 adopting an alternative conformation that effectively reduces the volume of the active site in this region. This feature is observed with each of the three biomimetics, with the remainder of the active site residues remaining static when compared to the NADPH<sub>4</sub> complex. The determined structures reveal that the biomimetic designs capture the design features of the natural coenzyme in that the nicotinamide moiety is positioned optimally over the *re*-face of the enzyme-bound FMN cofactor for hydride transfer from the C4 atom of the biomimetic to the N5 atom of the flavin isoalloxazine.

**Enzyme Reduction by Coenzyme Biomimetics.** In ERs, hydride transfer from the natural coenzyme to the flavin mononucleotide cofactor occurs by quantum mechanical tunnelling. The probability of hydride transfer by quantum mechanical tunnelling is affected by sub-angstrom changes in donor–acceptor distance.<sup>39–41</sup> Although the nicotinamide synthetic analogues and the natural coenzyme bind to the ER

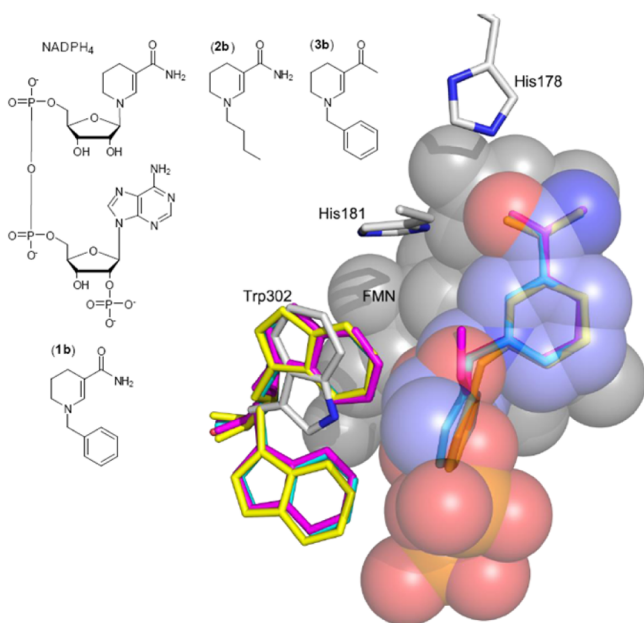


**Figure 2.** Superimposition showing the highly conserved nature of ligand and biomimetic binding. Structures cocrystallized in the presence of NADPH<sub>4</sub> and biomimetic compounds **1b**, **2b**, and **3b** are shown, superimposed based upon secondary structure elements using SSM (Coot).<sup>38</sup> Residues Trp302, His181, and His178 are shown in stick representation colored with white carbon atoms and blue nitrogen atoms. These residues correspond to the NADPH<sub>4</sub>-bound structure. The ordered portion of the NADPH<sub>4</sub> is shown as semitransparent spheres in all-atom color (carbon, purple; oxygen, red; phosphorus, orange) with its associated underlying FMN cofactor shown as gray spheres. Three biomimetic compounds are shown in stick representation with their respective Trp302 residues colored to match the biomimetic. **1b**, cyan; **2b**, yellow; and **3b**, magenta. Dual occupancies are present for residue Trp302 for each of the three mimics, indicating that occupancy is less than 100% for these compounds.

active site with similar geometry, subtle changes in the binding mode will influence the kinetics of hydride transfer. We determined the catalytic parameters for the reductive half-reaction (Figure 1B) for four ERs, namely, PETNR, TOYE, XenA, and TsOYE, using anaerobic rapid mixing stopped-flow measurements, employing the natural coenzymes NAD(P)H and the mNADH biomimetics (1–5) (Figure 1A).

Table 1 reports the reaction rates ( $k_{\text{red}}$ ) and the apparent dissociation constants ( $K_{\text{D}}$ ) for flavin reduction. Most ERs possess a higher affinity for the natural coenzyme NADPH compared to that for NADH.<sup>42,37,43,44</sup> This affinity is evident from the values of the apparent dissociation constants ( $K_{\text{D}}$ ) calculated from stopped-flow studies that differ by about an order of magnitude for all ERs investigated. The exception is TsOYE, with which the  $K_{\text{D}}$  values are essentially the same with both coenzymes. Furthermore, the values of the kinetic constants for the reductive half-reaction (i.e., hydride transfer;  $k_{\text{red}}$ ) depend on the type of natural coenzyme employed. The  $k_{\text{red}}$  values differed from 10- to 36-fold higher when using NADPH compared to that using NADH. In particular, PETNR shows significantly higher  $K_{\text{D}}$  values compared to those of the other ERs, and it is the only enzyme where  $k_{\text{red}}/K_{\text{D}}$  is 2 orders of magnitude higher for NADPH compared to that for NADH. With PETNR, the faster rates of flavin reduction with NADPH compared to that with NADH have been attributed to

**Table 1. Kinetic Parameters for the Reductive Half-Reaction of ERs with Natural and Biomimetic Coenzymes<sup>a</sup>**

coenzyme	PETNR			TOYE			XenA			TsOYE		
	$k_{\text{red}}$ [ $\text{s}^{-1}$ ]	$K_{\text{D}}$ [ $\mu\text{M}$ ]	$k_{\text{red}}/K_{\text{D}}$ [ $\text{mM}^{-1}\text{s}^{-1}$ ]	$k_{\text{red}}$ [ $\text{s}^{-1}$ ]	$K_{\text{D}}$ [ $\mu\text{M}$ ]	$k_{\text{red}}/K_{\text{D}}$ [ $\text{mM}^{-1}\text{s}^{-1}$ ]	$k_{\text{red}}$ [ $\text{s}^{-1}$ ]	$K_{\text{D}}$ [ $\mu\text{M}$ ]	$k_{\text{red}}/K_{\text{D}}$ [ $\text{mM}^{-1}\text{s}^{-1}$ ]	$k_{\text{red}}$ [ $\text{s}^{-1}$ ]	$K_{\text{D}}$ [ $\mu\text{M}$ ]	$k_{\text{red}}/K_{\text{D}}$ [ $\text{mM}^{-1}\text{s}^{-1}$ ]
NADPH	31 ± 0.2	202 ± 5	153	57 ± 0.5	5 ± 0.7	11 400	67 ± 2	27 ± 2	2481	47 ± 0.5	9 ± 0.6	5222
NADH	3 ± 0.1	1457 ± 12	2	4 ± 1	21 ± 0.5	191	3 ± 0.1	112 ± 6	27	1.3 ± 0.01	8 ± 0.7	163
<b>1</b>	19 ± 0.3	95 ± 4	200	236 ± 4	560 ± 18	421	68 ± 1	<25 <sup>b</sup>	>2720 <sup>b</sup>	121 ± 2	227 ± 5	533
<b>2</b>	120 ± 6	184 ± 15	652	386 ± 3	644 ± 9	600	388 ± 7	8 ± 1	48 500	147 ± 1	406 ± 12	362
<b>3</b>	17 ± 8	1625 ± 95	11	321 ± 25	2672 ± 150	120	117 ± 2	16 ± 1	7313	158 ± 3	917 ± 25	172
<b>4</b>	25 ± 1	1040 ± 67	24	770 ± 49	188 ± 23	4096	> 550 <sup>c</sup>	>>70 <sup>c</sup>		> 500 <sup>c</sup>	>>50 <sup>c</sup>	
<b>5</b>	n.d.	n.d.	n.d.	n.d.	n.d.	n.d.	0.08 ± 0.001	41 ± 3	2	n.d.	n.d.	n.d.

<sup>a</sup> $k_{\text{red}}$ , reaction rates [ $\text{s}^{-1}$ ];  $K_{\text{D}}$ , dissociation constants [ $\mu\text{M}$ ]; n.d., not determined due to poor conversion in biocatalytic reactions. Values obtained are an average of 5–6 shots. Reaction conditions: [ER] = 8–10  $\mu\text{M}$ , buffer 50 mM MOPS (pH 7.0) + 5 mM CaCl<sub>2</sub>, at 30 °C, under anaerobic conditions with constant N<sub>2</sub> flow, [coenzyme] = varied. <sup>b</sup>Not possible to measure at lower concentrations of the coenzyme due to non-pseudo-first-order conditions. <sup>c</sup>Rate of reduction occurs within the dead time of the stopped-flow instrument at higher concentrations of coenzyme.



Table 2. Steady-State Kinetics for ERs with 2-Cyclohexen-1-one and Varied Concentrations of NAD(P)H and mNADHs<sup>a</sup>

coenzyme	PETNR <sup>b</sup>			TOYE <sup>c</sup>			XenA <sup>d</sup>		
	$k_{app}$ [s <sup>-1</sup> ]	$K_M$ [ $\mu$ M]	$k_{app}/K_M$ [mM <sup>-1</sup> ·s <sup>-1</sup> ]	$k_{app}$ [s <sup>-1</sup> ]	$K_M$ [ $\mu$ M]	$k_{app}/K_M$ [mM <sup>-1</sup> ·s <sup>-1</sup> ]	$k_{app}$ [s <sup>-1</sup> ]	$K_M$ [ $\mu$ M]	$k_{app}/K_M$ [mM <sup>-1</sup> ·s <sup>-1</sup> ]
NADPH	8 ± 0.1	164 ± 7	49	15 ± 1	5 ± 1	3000	9 ± 0.3	13 ± 1.1	692
NADH	>1.2	>2500		3 ± 0.1	38 ± 3	79	2 ± 0.1	356 ± 17	6
1	5 ± 0.1	71 ± 5	70	23 ± 0.8	352 ± 40	65	13 ± 0.2	<7	>1857
2	11 ± 0.3	43 ± 3	256	21 ± 0.8	221 ± 25	95	21 ± 0.5	2 ± 0.5	10 500
3	10 ± 0.6	2035 ± 226	5	26 ± 3	1010 ± 174	26	13 ± 0.2	8 ± 0.3	1625

<sup>a</sup>Reaction conditions: buffer 50 mM MOPS (pH 7.0) + 5 mM CaCl<sub>2</sub>, at 30 °C, under anaerobic conditions with constant N<sub>2</sub> flow. [coenzyme] = varied, [ER] = 100–250 nM;  $\epsilon_{(mNADHs)}$ , see the Supporting Information. <sup>b</sup>[2-Cyclohexen-1-one] = 5.5 mM. <sup>c</sup>[2-Cyclohexen-1-one] = 35 mM. <sup>d</sup>[2-Cyclohexen-1-one] = 1.5 mM.

Table 3. Conversions [%] of 6 Reduced to (R)-6a by Various ERs with Different Coenzymes<sup>a</sup>

coenzyme	PETNR	TOYE	OYE2	OYE3	XenA	XenB	LeOPR1	NerA	MR	TsOYE	DrOYE	RmOYE
NADH	93	56	92	83	91	93	95	89	81	92	53	63
NADH <sup>b</sup>	28	>99	>99	62	99	>99	>99	>99	>99	n.d. <sup>c</sup>	n.d.	n.d.
NADPH	93	50	59	58	88	96	90	86	34	>99	64	45
NADPH <sup>b</sup>	>99	>99	>99	79	>99	>99	>99	>99	>99	n.d.	n.d.	n.d.
1	92	90	42	11	74	91	85	84	26	>99	>99	>99
2	70	59	25	10	63	75	66	67	29	>99	98	74
3	98	70	11	2	75	71	92	87	20	>99	>99	38
4	50	61	23	11	64	25	52	36	6	>99	>99	>99
5	2	10	1	1	80	1	3	2	4	59	9	43

<sup>a</sup>Reaction conditions: [6] = 10 mM, [ER] = 3.0–5.0  $\mu$ M, [coenzyme] = 11 mM (unless otherwise specified), MOPS buffer (50 mM, pH 7.0, 5 mM CaCl<sub>2</sub>), inert atmosphere, 30 °C, 4 h; the mNADHs were directly added as solids. Conversion was determined by GC. <sup>b</sup>GDH/glucose recycling system used. <sup>c</sup>n.d., not determined.

promoting vibrations that couple to the reaction coordinate and modulate the donor–acceptor distance for hydride tunneling.<sup>41,45</sup>

The rates of the reductive half-reactions were elevated using the nicotinamide biomimetic **2** compared to that using NADPH for each of the four ERs investigated. Additionally, biomimetic **2** binds with apparent higher affinity to the active site of the ERs compared with that of NADPH in two cases out of four, namely, with PETNR and XenA ( $K_D$  184 and 8  $\mu$ M, respectively). As a consequence, the  $k_{red}/K_D$  values for the reductive half-reaction of PETNR and XenA with the synthetic biomimetic **2** indicate superior catalytic efficiency compared to that of reactions with NADPH. The highest  $k_{red}/K_D$  value of 48 500 mM<sup>-1</sup> s<sup>-1</sup> was obtained employing biomimetic **2** with XenA, and to the best of our knowledge, this is the first report of a nicotinamide biomimetic surpassing the efficiency of natural coenzymes. The highest flavin reduction rates were obtained with biomimetic **4**. Biomimetic **4** harbors an acid group instead of the amide group in the nicotinamide moiety. The  $k_{red}$  values were higher than 500 s<sup>-1</sup> with XenA and TsOYE and reached a maximum of 770 s<sup>-1</sup> with TOYE.

Further detailed analysis is reported in Table 1, which indicates that each biomimetic performed better than NADH in reactions with PETNR (i.e., higher reaction rates; apparent dissociation constants were similar for the biomimetic and NADH). A similar trend was observed in hydride transfer reactions mediated by TOYE. In this case, the  $k_{red}$  values were elevated for all of the biomimetics when compared to those for both natural coenzymes. With that said, the ratio  $k_{red}/K_D$  was always in favor of the natural coenzymes due to the modest binding affinity of TOYE for the synthetic biomimetics. XenA stands apart from the other ERs: XenA was the only enzyme capable of catalyzing the reduction of an activated alkene using biomimetic **5** (see Enzyme-Catalyzed Redox Reactions Using

Coenzyme Biomimetics). Biomimetic **5** differs from the others in that it possesses a nitrile instead of carbonyl moiety, and kinetic parameters for the reaction of biomimetic **5** with XenA were determined. The  $K_D$  values for the reduction with **5** and NADPH with XenA are similar, whereas  $k_{red}$  differs by 3 orders of magnitude (i.e., 0.08 and 67 s<sup>-1</sup> for **5** and NADPH, respectively). In general, the highest reaction rate with XenA was obtained using biomimetic **4**, whereas three biomimetics (**1**, **2**, and **3**) showed a higher apparent affinity compared with that of the natural coenzymes. Reactions with TsOYE confirmed the general trend, i.e., increased reaction rates with the biomimetics but elevated  $K_D$  values for the enzyme–biomimetic complex compared to values measured with the natural coenzymes.

**Steady-State Kinetics.** ERs catalyze the reduction of activated alkenes following a ping-pong bi-bi mechanism.<sup>42,46–48</sup> Stopped-flow experiments demonstrated that reductive rates are higher for a number of nicotinamide biomimetics than for natural coenzymes, but in order to obtain better insight into the overall catalytic cycle (relevant to exploitation of any ER with a coenzyme biomimetic in biocatalysis), steady-state kinetic investigations were undertaken studying three ERs, namely, PETNR, TOYE, and XenA. In each case, 2-cyclohexen-1-one was used as the second substrate in reactions employing NAD(P)H and the biomimetics. For many ERs the oxidative half-reaction limits the overall kinetics of the complete catalytic cycle,<sup>39,49</sup> and the  $k_{app}$  values were similar when using NADPH or the synthetic biomimetics. Only the use of NADH led to a slight deviation from this trend (Table 2). Again, biomimetic **2** is of particular interest as it gave the highest ratio of  $k_{app}/K_M$  in two cases out of three (i.e., PETNR, XenA), confirming that this synthetic analogue has an improved catalytic efficiency compared to that with NADPH.

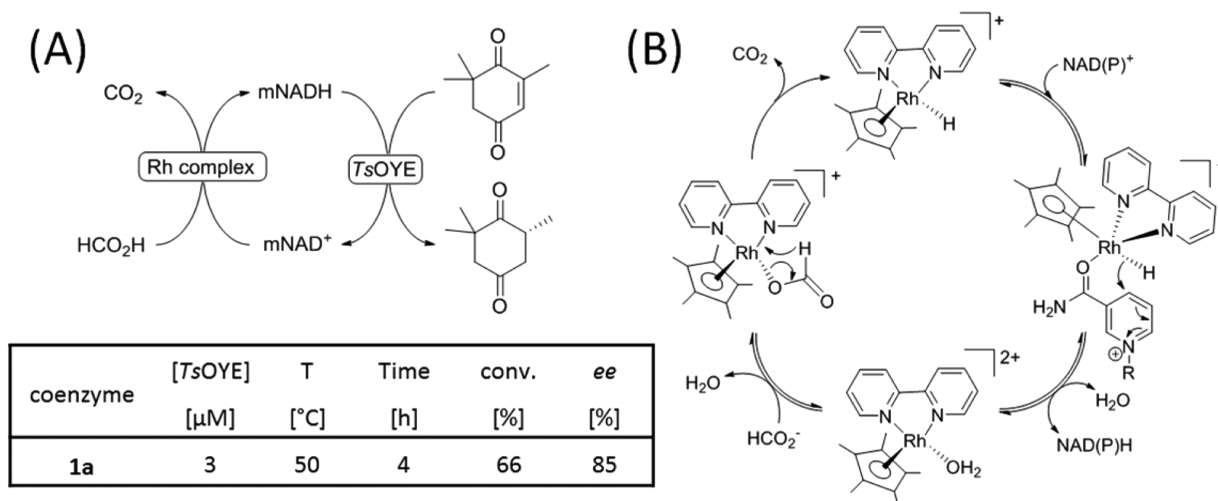


**Figure 3.** (A) Investigated recycling system of mNADHs with *TsOYE* and the rhodium complex  $[\text{Cp}^*\text{Rh}(\text{bpy})(\text{H}_2\text{O})]^{2+}$ . The nicotinamide coenzyme mimic  $\text{mNAD}^+$  is reduced by  $[\text{Cp}^*\text{Rh}(\text{bpy})(\text{H}_2\text{O})]^{2+}$ . Reaction conditions:  $[\mathbf{6}] = 10 \text{ mM}$ ,  $[\text{ER}] = 3.0 \mu\text{M}$ ,  $[\text{oxidized coenzyme } \mathbf{1a}] = 1 \text{ mM}$ ,  $[\text{NaHCO}_2] = 60 \text{ mM}$ ,  $[\text{Rh complex}] = 0.25 \text{ mM}$ , MOPS buffer (50 mM, pH 7.0, 5 mM  $\text{CaCl}_2$ ), inert atmosphere, 50 °C, 4 h; the mNADHs were directly added as solids. Conversion was determined by GC. (B) Proposed mechanism for the reduction of  $\text{NAD}(\text{P})^+$  by  $[\text{Cp}^*\text{Rh}(\text{bpy})(\text{H}_2\text{O})]^{2+}$ .<sup>51</sup> The table shows that 66% conversion could be obtained after 4 h reaction time.

**Enzyme-Catalyzed Redox Reactions Using Coenzyme Biomimetics.** Our previous study revealed that biomimetic coenzymes **1–5** are readily accepted by the ERs from *Thermus scotoductus* (*TsOYE*) and *Bacillus subtilis* (*YqjM*). To evaluate whether this was generally the case for all of the members of the ER family, we investigated a more representative selection of ERs. We carried out the asymmetric reduction of ketoisophorone **6** to levodione (*R*)-**6a** using an extended panel of 12 ERs from the OYE family (PETNR, TOYE, OYE2, OYE3, XenA, XenB, LeOPRI, NerA, MR, *TsOYE*, *DrOYE*, and *RmOYE*) and the five biomimetics (**1–5**). The results in Table 3 show that the biomimetics were overall well-accepted, leading up to quantitative conversions, with the exception of mNADH **5**. In fact, XenA was the only enzyme that efficiently accepted mNADH **5** as the hydride source. This finding is in line with the kinetic parameters shown in Tables 1 and 2. As expected, the source of hydride, whether from the natural or synthetic coenzyme, did not have a significant influence on the enantiomeric excess (Table S3, Supporting Information), which is dependent on the intrinsic stereoselectivity of the enzyme only. The slight deviations in the enantiomeric excess are due to the slow spontaneous racemization of the product in aqueous medium.<sup>50</sup>

**Recycling of Coenzyme Biomimetics.** The biocatalytic reduction described in the previous section was carried out at the expense of stoichiometric amounts of nicotinamide biomimetic as hydride donor, which is a limitation in developing inexpensive biocatalytic transformations. The rhodium complex  $[\text{Cp}^*\text{Rh}(\text{bpy})(\text{H}_2\text{O})]^{2+}$  is capable of reducing biomimetics **1** and **3** using formate as a hydride source.<sup>51</sup> Hence, to use the biomimetics in catalytic amounts, we implemented a recycling system for the ER-catalyzed reduction of **6** to (*R*)-**6a**, as depicted in Figure 3A. The reduced form of the Rh-catalyst binds the carbonyl moiety of the oxidized form of the biomimetic, followed by hydride transfer from the metal center to the aromatic ring of the biomimetic. After the release of the reduced mimic from the metal center, the organometallic catalyst is reduced back at the expense of formate, which is oxidized to  $\text{CO}_2$ . After a preliminary

optimization of the reaction conditions (see the Supporting Information for more details),<sup>52</sup> the reduction of ketoisophorone **6** was performed with *TsOYE*, oxidized biomimetic **1a**, and the rhodium complex  $[\text{Cp}^*\text{Rh}(\text{bpy})(\text{H}_2\text{O})]^{2+}$ , using sodium formate as the hydride donor. Under these reaction conditions (see the Supporting Information for more details), 6.6 mM product with an ee of 85% was obtained starting with 1 mM **1a**. Therefore, an in situ recycling method for  $\text{mNAD}^+$  **1a** with an ER was demonstrated.

**Extending the Application of Coenzyme Biomimetics in Biocatalysis beyond Ene-Reductases and Flavin Enzymes.** The structural, kinetic, and biocatalytic studies of the biomimetics with a wide range of ER enzymes demonstrate that they faithfully capture, at the functional level, design aspects inferred from the structures of the natural coenzymes and the natural coenzyme–ER protein complexes. That the biomimetics are also stable and can be recycled in biocatalytic transformations is important for applications in white biotechnology. The general utility of these synthetic biomimetics beyond the ER family is also important in adopting their use more widely in biocatalytic manufacture. We tested various  $\text{NAD}(\text{P})\text{H}$ -dependent oxidoreductases with the five synthetic biomimetics. Enzymes were chosen to encompass some of the most useful transformations for the manufacture of chemical products such as the monooxygenation of unfunctionalized carbon–hydrogen bonds or of ketones to esters, the chemoselective reduction of carboxylic acids to aldehydes and the reverse reaction, the reductive amination of ketones, the reduction of alkenes using non-flavin-dependent enzymes, and the regeneration of the oxidized form of the biomimetics. Activity assays using the non-flavin-dependent double-bond reductase from *Nicotiana tabacum* (*NtDBR*)<sup>15</sup> showed that the biomimetics also support the reduction of cinnamaldehyde to hydro-cinnamaldehyde at the expense of biomimetics **1–4**, with conversion ranging from 5 to 21%. Further kinetic data (see the Supporting Information for more details) showed that *NtDBR* has the highest preference for NADPH as the hydride donor for the reduction of cinnamaldehyde ( $k_{\text{cat}} 40 \text{ min}^{-1}$ ,  $K_M 91 \mu\text{M}$ ). Conversely, the observed rate measured at 5 mM substrate

concentration revealed a reduced turnover number for NADH ( $k_{\text{obs}} 4 \text{ min}^{-1}$ ) as well as biomimetics **1** ( $k_{\text{obs}} 0.15 \text{ min}^{-1}$ ) and **3** ( $k_{\text{obs}} 0.08 \text{ min}^{-1}$ ).

Additionally, a NADPH oxidase isolated from *B. subtilis*<sup>53,54</sup> was also capable of efficiently oxidizing biomimetics **1–4** using molecular oxygen as the only electron acceptor. These are examples that demonstrate the versatility of the cofactor analogues in addition to the previously established system with a styrene monooxygenase, greatly improving the efficiency of electron transfer for the selective epoxidation of styrene derivatives.<sup>32</sup> It seems logical that structural knowledge of natural/biomimetic coenzyme–biocatalyst complexes, similar to that described herein, will guide further design of new biomimetics, extending their reach to other useful transformations. This should extend the biomimetic series beyond compounds **1–5** and enable widespread application of nicotinamide biomimetics in biocatalytic processes.

## CONCLUDING REMARKS

We have shown that synthetic coenzyme biomimetics can outperform natural coenzymes in biotransformations reactions with widely used redox biocatalysts. That laboratory-based designs can outperform those available in Nature is notable. These synthetic coenzymes are inexpensive to manufacture, are stable relative to their biological counterparts, and are operational with a wide range of biocatalysts taken from the ER family and a few other oxidoreductases. Additionally, the biomimetics can be recycled at the expense of formate and are therefore exploitable using only catalytic amounts. Implementation of these synthetic biomimetics as well as the design of more sophisticated analogues capable of operating with a variety of other oxidoreductases will facilitate the use of redox biocatalysts in chemicals production at low cost and thereby transform the use of oxidoreductases more widely in industrial biocatalysis.

## ASSOCIATED CONTENT

### Supporting Information

The Supporting Information is available free of charge on the ACS Publications website at DOI: 10.1021/jacs.5b12252.

Experimental details including the synthesis of mNADHs, mNADs, mNADH<sub>4</sub>s, overexpression of the enzymes, determination of the molar extinction coefficient for mNADHs, reductive half-reaction data, steady-state kinetic data, biocatalytic transformations, recycling of mNAD<sup>+</sup>, and crystallization experiments (PDF)

## AUTHOR INFORMATION

### Corresponding Authors

\*f.hollmann@tudelft.nl (F.H.)

\*nigel.scrutton@manchester.ac.uk (N.S.S.)

### Present Address

<sup>||</sup>(T.K. and F.G.M.) Van't Hoff Institute for Molecular Sciences, University of Amsterdam, Science Park 904, 1098 XH Amsterdam, The Netherlands.

### Author Contributions

<sup>§</sup>T.K. and C.E.P. contributed equally to this work.

### Notes

The authors declare no competing financial interest.

## ACKNOWLEDGMENTS

This work was supported by the Marie Curie IEF “Biomimic” financed by the European Union through the seventh Framework People Programme (grant agreement number 327647) and by the UK Biotechnology and Biological Sciences Research Council (BBSRC; BB/K0017802/1) and GlaxoSmithKline. N.S.S. received funding as an Engineering and Physical Sciences Research Council (EPSRC) Established Career Fellow (EP/J020192/1) and a Royal Society Wolfson Merit Award. F.G.M. received funding as a European Research Council (ERC) Starting Grant Fellow (H2020, grant agreement 638271, BioSusAmin). The BBSRC (BB/M017702/1) supported infrastructure for analytical chemistry. Marc J. F. Strampraad is gratefully acknowledged for his technical assistance. We thank Luke Humphreys (GlaxoSmithKline) and Gideon J. Grogan for fruitful discussions and Diederik J. Opperman for providing *DrOYE* and *RmOYE*. Furthermore, we thank Diamond Light Source for access to beamlines i02 and i03 (MX8997) that contributed to the results presented here. The authors thank Verena Resch for her great artwork in the graphical abstract.

## REFERENCES

- (1) Toogood, H. S.; Knaus, T.; Scrutton, N. S. *ChemCatChem* **2014**, *6*, 951.
- (2) Taglieber, A.; Schulz, F.; Hollmann, F.; Rusek, M.; Reetz, M. T. *ChemBioChem* **2008**, *9*, 565.
- (3) Grau, M. M.; van der Toorn, J. C.; Otten, L. G.; Macheroux, P.; Taglieber, A.; Zilly, F. E.; Arends, I. W. C. E.; Hollmann, F. *Adv. Synth. Catal.* **2009**, *351*, 3279.
- (4) Hollmann, F.; Arends, I. W. C. E.; Buehler, K. *ChemCatChem* **2010**, *2*, 762.
- (5) Fisher, K.; Mohr, S.; Mansell, D.; Goddard, N. J.; Fielden, P. R.; Scrutton, N. S. *Catal. Sci. Technol.* **2013**, *3*, 1505.
- (6) Knaus, T.; Mutti, F. G.; Humphreys, L. D.; Turner, N. J.; Scrutton, N. S. *Org. Biomol. Chem.* **2015**, *13*, 223.
- (7) Schrittwieser, J. H.; Sattler, J.; Resch, V.; Mutti, F. G.; Kroutil, W. *Curr. Opin. Chem. Biol.* **2011**, *15*, 249.
- (8) Sattler, J. H.; Fuchs, M.; Tauber, K.; Mutti, F. G.; Faber, K.; Pfeffer, J.; Haas, T.; Kroutil, W. *Angew. Chem., Int. Ed.* **2012**, *51*, 9156.
- (9) Gargiulo, S.; Opperman, D. J.; Hanefeld, U.; Arends, I. W. C. E.; Hollmann, F. *Chem. Commun.* **2012**, *48*, 6630.
- (10) Paul, C. E.; Gargiulo, S.; Opperman, D. J.; Lavandera, I.; Gotor-Fernandez, V.; Gotor, V.; Taglieber, A.; Arends, I. W. C. E.; Hollmann, F. *Org. Lett.* **2013**, *15*, 180.
- (11) Toogood, H. S.; Gardiner, J. M.; Scrutton, N. S. *ChemCatChem* **2010**, *2*, 892.
- (12) Stuermer, R.; Hauer, B.; Hall, M.; Faber, K. *Curr. Opin. Chem. Biol.* **2007**, *11*, 203.
- (13) Toogood, H. S.; Scrutton, N. S. *Curr. Opin. Chem. Biol.* **2014**, *19*, 107.
- (14) Fu, Y.; Castiglione, K.; Weuster-Botz, D. *Biotechnol. Bioeng.* **2013**, *110*, 1293.
- (15) Mansell, D. J.; Toogood, H. S.; Waller, J.; Hughes, J. M. X.; Levy, C. W.; Gardiner, J. M.; Scrutton, N. S. *ACS Catal.* **2013**, *3*, 370.
- (16) Burda, E.; Röss, T.; Winkler, T.; Giese, C.; Kostrov, X.; Huber, T.; Hummel, W.; Groger, H. *Angew. Chem., Int. Ed.* **2013**, *52*, 9323.
- (17) Yanto, Y.; Yu, H. H.; Hall, M.; Bommarius, A. S. *Chem. Commun.* **2009**, *46*, 8809.
- (18) Stueckler, C.; Hall, M.; Ehammer, H.; Pointner, E.; Kroutil, W.; Macheroux, P.; Faber, K. *Org. Lett.* **2007**, *9*, 5409.
- (19) Tasnadi, G.; Winkler, C. K.; Clay, D.; Sultana, N.; Fabian, W. M. F.; Hall, M.; Ditrich, K.; Faber, K. *Chem. - Eur. J.* **2012**, *18*, 10362.
- (20) Brenna, E.; Gatti, F. G.; Manfredi, A.; Monti, D.; Parmeggiani, F. *Eur. J. Org. Chem.* **2011**, *2011*, 4015.

- (21) Tasnádi, G.; Winkler, C. K.; Clay, D.; Hall, M.; Faber, K. *Catal. Sci. Technol.* **2012**, *2*, 1548.
- (22) Stueckler, C.; Winkler, C. K.; Bonnekessel, M.; Faber, K. *Adv. Synth. Catal.* **2010**, *352*, 2663.
- (23) Stueckler, C.; Mueller, N. J.; Winkler, C. K.; Glueck, S. M.; Gruber, K.; Steinkellner, G.; Faber, K. *Dalton transactions* **2010**, *39*, 8472.
- (24) Brenna, E.; Gatti, F. G.; Malpezzi, L.; Monti, D.; Parmeggiani, F.; Sacchetti, A. J. *Org. Chem.* **2013**, *78*, 4811.
- (25) Brenna, E.; Gatti, F. G.; Manfredi, A.; Monti, D.; Parmeggiani, F. *Org. Process Res. Dev.* **2012**, *16*, 262.
- (26) Winkler, C. K.; Tasnadi, G.; Clay, D.; Hall, M.; Faber, K. J. *J. Biotechnol.* **2012**, *162*, 381.
- (27) Toogood, H.; Mansell, D.; Gardiner, J. M.; Scrutton, N. S. *Comprehensive Chirality* **2012**, *1*, 216.
- (28) Kohli, R. M.; Massey, V. J. *Biol. Chem.* **1998**, *273*, 32763.
- (29) Brown, B. J.; Deng, Z.; Karplus, P. A.; Massey, V. J. *Biol. Chem.* **1998**, *273*, 32753.
- (30) Pudney, C. R.; Hay, S.; Scrutton, N. S. *FEBS J.* **2009**, *276*, 4780.
- (31) Paul, C. E.; Arends, I. W. C. E.; Hollmann, F. *ACS Catal.* **2014**, *4*, 788.
- (32) Paul, C. E.; Tischler, D.; Riedel, A.; Heine, T.; Itoh, N.; Hollmann, F. *ACS Catal.* **2015**, *5*, 2961.
- (33) Ryan, J. D.; Fish, R. H.; Clark, D. S. *ChemBioChem* **2008**, *9*, 2579.
- (34) Paul, C. E.; Churakova, E.; Maurits, E.; Girhard, M.; Urlacher, V. B.; Hollmann, F. *Bioorg. Med. Chem.* **2014**, *22*, 5692.
- (35) Lutz, J.; Hollmann, F.; Ho, T. V.; Schnyder, A.; Fish, R. H.; Schmid, A. J. *J. Organomet. Chem.* **2004**, *689*, 4783.
- (36) Fox, K. M.; Karplus, P. A. *Structure* **1994**, *2*, 1089.
- (37) Adalbjornsson, B. V.; Toogood, H. S.; Fryszkowska, A.; Pudney, C. R.; Jowitt, T. A.; Leys, D.; Scrutton, N. S. *ChemBioChem* **2010**, *11*, 197.
- (38) Krissinel, E.; Henrick, K. *Acta Crystallogr., Sect. D: Biol. Crystallogr.* **2004**, *60*, 2256.
- (39) Basran, J.; Harris, R. J.; Sutcliffe, M. J.; Scrutton, N. S. *J. Biol. Chem.* **2003**, *278*, 43973.
- (40) Pudney, C. R.; Hay, S.; Sutcliffe, M. J.; Scrutton, N. S. *J. Am. Chem. Soc.* **2006**, *128*, 14053.
- (41) Pudney, C. R.; Hay, S.; Levy, C.; Pang, J.; Sutcliffe, M. J.; Leys, D.; Scrutton, N. S. *J. Am. Chem. Soc.* **2009**, *131*, 17072.
- (42) French, C. E.; Nicklin, S.; Bruce, N. C. *J. Bacteriol.* **1996**, *178*, 6623.
- (43) Chaparro-Riggers, J. F.; Rogers, T. A.; Vazquez-Figueroa, E.; Polizzi, K. M.; Bommarius, A. S. *Adv. Synth. Catal.* **2007**, *349*, 1521.
- (44) Fitzpatrick, T. B.; Amrhein, N.; Macheroux, P. *J. Biol. Chem.* **2003**, *278*, 19891.
- (45) Pudney, C. R.; Lane, R. S. K.; Fielding, A. J.; Magennis, S. W.; Hay, S.; Scrutton, N. S. *J. Am. Chem. Soc.* **2013**, *135*, 3855.
- (46) Karplus, P. A.; Fox, K. M.; Massey, V. *FASEB J.* **1995**, *9*, 1518.
- (47) French, C. E.; Bruce, N. C. *Biochem. J.* **1994**, *301*, 97.
- (48) Nivinskas, H.; Sarlauskas, J.; Anusevicius, Z.; Toogood, H. S.; Scrutton, N. S.; Cenas, N. *FEBS J.* **2008**, *275*, 6192.
- (49) Niino, Y. S.; Chakraborty, S.; Brown, B. J.; Massey, V. *J. Biol. Chem.* **1995**, *270*, 1983.
- (50) Fryszkowska, A.; Toogood, H.; Sakuma, M.; Gardiner, J. M.; Stephens, G. M.; Scrutton, N. S. *Adv. Synth. Catal.* **2009**, *351*, 2976.
- (51) Lo, H. C.; Buriez, O.; Kerr, J. B.; Fish, R. H. *Angew. Chem., Int. Ed.* **1999**, *38*, 1429.
- (52) Bernard, J.; van Heerden, E.; Arends, I. W. C. E.; Opperman, D. J.; Hollmann, F. *ChemCatChem* **2012**, *4*, 196.
- (53) Morokutti, A.; Lyskowski, A.; Sollner, S.; Pointner, E.; Fitzpatrick, T. B.; Kratky, C.; Gruber, K.; Macheroux, P. *Biochemistry* **2005**, *44*, 13724.
- (54) Voss, C. V.; Gruber, C. C.; Faber, K.; Knaus, T.; Macheroux, P.; Kroutil, W. *J. Am. Chem. Soc.* **2008**, *130*, 13969.